

# About an inverse electromagnetic coefficient problem: uniqueness with partial boundary data and quasi-reversibility method for data completion

Marion Darbas<sup>a</sup>      Jérémy Heleine<sup>b</sup>      Stephanie Lohrengel<sup>c</sup>

Drafted 25 October 2019

## Abstract

This paper deals with two questions relative to the inverse coefficient problem of recovering the electric permittivity and conductivity of a medium from partial boundary data at a fixed frequency. The underlying model is the time-harmonic Maxwell equations in the electric field. First, an identifiability result is proved for partial boundary data without restrictive conditions on the inaccessible part of the boundary. The second issue that is addressed, is the data completion problem on the inaccessible part of the boundary. The quasi-reversibility method is studied, and different mixed formulations are proposed. Well-posedness and convergence results are proved. Various two- and three dimensional numerical simulations attest the efficiency of the method, in particular for noisy data.

**Keywords:** Maxwell equations, inverse medium problem, identifiability, data completion, quasi-reversibility method

## 1 Introduction

Let  $\Omega$  denote a bounded and simply connected domain in  $\mathbb{R}^d$ ,  $d = 2, 3$  of boundary  $\Gamma := \partial\Omega$ . The unit outward normal to  $\Omega$  is denoted by  $\mathbf{n}$ . Assume the medium in  $\Omega$  to be inhomogeneous and isotropic, of constant magnetic permeability  $\mu = \mu_0$  with  $\mu_0$  the magnetic permeability in vacuum. Let  $\varepsilon, \sigma$  be non-negative functions representing the electric permittivity and conductivity respectively. The refractive index  $\kappa$  of the medium in  $\Omega$  is defined by  $\kappa(\mathbf{x}) = \frac{1}{\varepsilon_0} \left( \varepsilon(\mathbf{x}) + i \frac{\sigma(\mathbf{x})}{\omega} \right)$ ,  $\mathbf{x} \in \Omega$ , where  $\varepsilon_0$  is the electric permittivity in vacuum. Consider the electric field intensity  $\mathbf{E}$  satisfying the time-harmonic Maxwell equations at a frequency  $\omega > 0$

$$\mathbf{curl} \mathbf{curl} \mathbf{E} - k^2 \kappa \mathbf{E} = 0, \quad \text{in } \Omega, \quad (1)$$

with Dirichlet or Neumann boundary condition on  $\Gamma$ . The number  $k := \omega \sqrt{\mu_0 \varepsilon_0}$  is the wavenumber. We are interested in the inverse boundary value problem of recovering the electric permittivity  $\varepsilon$  and conductivity  $\sigma$  from partial boundary data on  $\Gamma$  at a fixed frequency  $\omega$ . The study of dielectric properties of biological tissues or materials is of great interest in medical or industrial applications. Information about the characteristics and composition of a tissue or a material can be used to develop

<sup>a</sup>Contact: marion.darbas@u-picardie.fr. LAMFA CNRS UMR 7352 - Université de Picardie Jules Verne, 33 rue Saint-Leu, 80039 Amiens cedex 1

<sup>b</sup>Contact: jeremy.heleine@u-picardie.fr. LAMFA CNRS UMR 7352 - Université de Picardie Jules Verne, 33 rue Saint-Leu, 80039 Amiens cedex 1

<sup>c</sup>Contact: stephanie.lohrengel@univ-reims.fr. LMR CNRS FRE2011 - Université de Reims Champagne-Ardenne, Moulin de la Housse, 51687 Reims cedex 2

new non-invasive modalities in many practical applications of electric fields in agriculture, bioengineering, geophysical exploration, and medical diagnosis. For instance, microwave imaging (electromagnetic high frequencies) is under investigation for cancer screening or brain stroke detection (see Tournier *et al* [35, 36]).

The fundamental example of coefficient reconstruction is Calderón’s inverse conductivity problem [14]. The theoretical and numerical study of Calderón’s problem in Electrical Impedance Tomography (which consists in reconstructing the conductivity of a medium from boundary measurements of electric voltages and currents) has also been extensively addressed in the last two decades. An important number of works have dealt with the questions of uniqueness, stability and reconstruction. Without being exhaustive, we refer for instance to [33, 1, 9, 37, 3, 16, 4] and references therein. In this paper, we focus on the inverse medium problem associated with the time-harmonic Maxwell equations formulated in the electric field. We are interested in particular in both the uniqueness question for partial data and the data completion problem. The two issues are complementary in view of the numerical coefficient reconstruction from measurements collected only on an accessible part of the boundary. The uniqueness issue aims to answer the (theoretical) question whether it is possible or not to recover the coefficients from the boundary data. In most configurations, one single measurement is not sufficient to identify the coefficient functions, and typical identifiability results state that identical Dirichlet-to-Neumann maps (on part of the boundary) yield identical coefficient functions. From a practical point of view, the knowledge of the complete Dirichlet-to-Neumann map is not realistic since it requires an infinite number of source terms. But the knowledge of a single couple of Dirichlet-Neumann data on part of the boundary only, leads to another difficulty: whereas the boundary data are over-determined on the accessible part, they are under-determined on the inaccessible part. Hence, the numerical resolution of the direct problem which is a crucial part in most identification or minimization algorithms, is not possible without an appropriate data completion procedure.

The usual inverse boundary value problem (IBVP) for the time-harmonic (full) Maxwell equations was first proposed in [32]. The lack of ellipticity of Maxwell’s equations adds complexities to the problem. We refer to the introduction of [17] which gives an interesting overview of the results related to the IBVP for Maxwell’s equations.

With regard to our first concern, two uniqueness results for certain types of partial data are stated in [15] and [13]. Their assumptions can be restrictive in the practical applications we have in mind: Caro [15] imposes some geometrical conditions on the inaccessible part of the boundary. Brown *et al* [13] consider a perfect conducting boundary condition on this part. We propose to fix neither geometrical nor boundary conditions.

As mentioned before, the data completion problem consists in recovering data on the inaccessible part of the boundary from measured data on the accessible part. The corresponding Cauchy problem is well-known to be ill-posed (e.g. [2, 7]). Different regularization methods have been introduced for reconstructing the missing data for elliptic equations (see e.g. [5, 6, 8, 27]). We focus on the non-iterative quasi-reversibility approach. It was introduced by Lattès and Lions [29]. The idea is to replace the ill-posed Cauchy problem with a family of well-posed variational problems with additional unknowns which depend on a small regularization parameter. The variational setting is numerically interesting since finite element methods can be used. The quasi-reversibility method has been successfully adopted and validated for Laplace’s equation [28, 10, 11, 22] and Helmholtz’s equation [12]. In the present paper, we study a quasi-reversibility method for the vector Maxwell equations. To the best of our knowledge, it’s the first time that such an approach is studied for solving a data completion problem in electromagnetics.

The article is organized as follows. Section 2 is devoted to the uniqueness result and its proof. Section 3 presents a first version of the quasi-reversibility method for solving the data completion problem for Maxwell’s equations in the electric field. Both theoretical and numerical aspects are addressed. Section 4 proposes two relaxed mixed problems with regularization in order to deal with noisy data. The relaxed problem is shown to be well posed, and convergence to the solution of the initial problem is proven under some conditions on the involved regularization and relaxation parameters. Numerical simulations confirm the theoretical results in two and three dimensions of space and attest

the efficiency of the method. Finally, we give some concluding remarks.

## 2 Uniqueness result

Let  $\Gamma_0$  be a non-empty open subset of  $\Gamma$ , called accessible part of  $\Gamma$  (see Definition 2.1) [13]. The inverse boundary value problem that we are interested in, is to determine the electric permittivity  $\varepsilon$  and conductivity  $\sigma$  from boundary measurements taken on  $\Gamma_0$  for a given (boundary) source term, at a fixed frequency  $\omega$ . These measurements together with the source term, define a Cauchy data set  $C(\varepsilon, \sigma; \Gamma_0)$  (see Definition 2.3) [17]. The uniqueness question reads as follows: Given a frequency  $\omega > 0$  and two sets of non-negative coefficients  $\{\varepsilon_j, \sigma_j\}$ ,  $j \in \{1, 2\}$ , does  $C(\varepsilon_1, \sigma_1; \Gamma_0) = C(\varepsilon_2, \sigma_2; \Gamma_0)$  imply  $\varepsilon_1 = \varepsilon_2$  and  $\sigma_1 = \sigma_2$  in  $\Omega$ ?

Two uniqueness results for partial data are stated in [15] and [13]. Caro imposes some geometrical conditions on the inaccessible part  $\Gamma_1$  which is supposed to be either part of a plane or part of a sphere [15]. Brown *et al* [13] relax this geometrical condition on  $\Gamma_1$  (the boundary of the domain is assumed  $C^{1,1}$ ) but consider a perfect conducting boundary condition  $\mathbf{E}|_{\Gamma_1} \times \mathbf{n} = 0$ . This hypothesis can be restrictive in applications. Our Theorem 2.4 can be seen as an improvement of these results. In our configuration, neither geometrical nor boundary conditions are fixed on  $\Gamma_1$ . The idea behind the proof of Theorem 2.4 is simple and new. It uses the unique continuation principle and results of Caro and Zhou [17].

Let us address the different definitions useful for our uniqueness result. Let us introduce the vector space  $H(\mathbf{curl}; \Omega) = \{\mathbf{u} \in L^2(\Omega)^3; \mathbf{curl} \mathbf{u} \in L^2(\Omega)^3\}$ . For any vector field  $\mathbf{u} \in H(\mathbf{curl}; \Omega)$ , we define the tangential trace by continuous extension of the mapping  $\gamma_t(\mathbf{u}) := \mathbf{u}|_{\Gamma} \times \mathbf{n}$ . We introduce the trace space  $Y(\Gamma) = \{\mathbf{f} \in H^{-1/2}(\Gamma)^3; \exists \mathbf{u} \in H(\mathbf{curl}; \Omega) / \gamma_t(\mathbf{u}) = \mathbf{f}\}$  and its restriction to  $\Gamma_0$  in the distributional sense  $Y(\Gamma_0) = \{\mathbf{f}|_{\Gamma_0}; \mathbf{f} \in Y(\Gamma)\}$ .

**Definition 2.1.** *Let  $\Omega$  be a non-empty, open, bounded connected domain in  $\mathbb{R}^3$  with Lipschitz boundary  $\Gamma$ . Let  $\Gamma_0$  a smooth non-empty open subset of  $\Gamma$  such that  $\text{meas } \Gamma_0 > 0$ . The part  $\Gamma_0$  is called the accessible part of the boundary  $\Gamma$  and  $\Gamma_1 := \Gamma \setminus \overline{\Gamma_0}$  the inaccessible part.*

The set of admissible coefficients  $\varepsilon$  and  $\sigma$  is given in the following definition.

**Definition 2.2.** *The pair of coefficients  $\varepsilon$  and  $\sigma$  is admissible if  $\varepsilon, \sigma \in C^1(\overline{\Omega})$  such that  $\varepsilon(\mathbf{x}) \geq \tilde{\varepsilon}$  and  $\sigma(\mathbf{x}) \geq 0$  almost everywhere in  $\Omega$  for a strictly positive constant  $\tilde{\varepsilon}$ .*

**Definition 2.3.** *Let  $\Omega$  and  $\Gamma_0$  be as in Definition 2.1. For a pair of admissible coefficients  $(\varepsilon, \sigma)$  defined on  $\Omega$  as in Definition 2.2, the corresponding Cauchy data set  $C(\varepsilon, \sigma; \Gamma_0)$  at a fixed frequency  $\omega > 0$  consists of pairs  $(\mathbf{f}, \mathbf{g}) \in Y(\Gamma_0) \times Y(\Gamma_0)$  such that there exists a solution  $\mathbf{E} \in H(\mathbf{curl}; \Omega)$  satisfying (1) for  $\kappa = (\varepsilon + i\sigma/\omega)/\varepsilon_0$ , and the boundary conditions  $\mathbf{E}|_{\Gamma_0} \times \mathbf{n} = \mathbf{f}$  and  $\mathbf{curl} \mathbf{E}|_{\Gamma_0} \times \mathbf{n} = \mathbf{g}$ .*

The definition of Cauchy data sets is used for instance in [25, 15, 17]. The partial boundary data are also given by the admittance map  $\Lambda: \mathbf{E}|_{\Gamma} \times \mathbf{n} \mapsto \mathbf{curl} \mathbf{E}|_{\Gamma} \times \mathbf{n}$  restricted to  $\Gamma_0$  if  $\omega$  is not a resonant frequency for (1). The uniqueness result reads as follows.

**Theorem 2.4.** *Let  $\Omega$  and  $\Gamma_0$  be as in Definition 2.1. Let  $\omega > 0$  a frequency. Assume that  $\varepsilon_j, \sigma_j$ ,  $j \in \{1, 2\}$ , are two pairs of admissible coefficients such that  $\varepsilon_1 = \varepsilon_2$  and  $\sigma_1 = \sigma_2$  in  $\overline{\mathcal{V}}$  where  $\mathcal{V}$  is a neighbourhood of  $\Gamma$ . Then,  $C(\varepsilon_1, \sigma_1; \Gamma_0) = C(\varepsilon_2, \sigma_2; \Gamma_0)$  implies  $\varepsilon_1 = \varepsilon_2$  and  $\sigma_1 = \sigma_2$  in  $\Omega$ .*

**Proof.** The proof is divided into two parts.

In a first step, we prove that the Cauchy data sets coincide not only on  $\Gamma_0$ , but on the whole boundary  $\Gamma$ . To this end, consider a couple  $(\mathbf{f}, \mathbf{g}) \in C(\varepsilon_1, \sigma_1; \Gamma)$ , and let  $\mathbf{E}_1 \in H(\mathbf{curl}; \Omega)$  satisfy

$$\begin{cases} \mathbf{curl} \mathbf{curl} \mathbf{E}_1 - k^2 \kappa_1 \mathbf{E}_1 = 0, & \text{in } \Omega, \\ \mathbf{E}_1 \times \mathbf{n} = \mathbf{f}, & \text{on } \Gamma, \\ \mathbf{curl} \mathbf{E}_1 \times \mathbf{n} = \mathbf{g}, & \text{on } \Gamma. \end{cases} \quad (2)$$

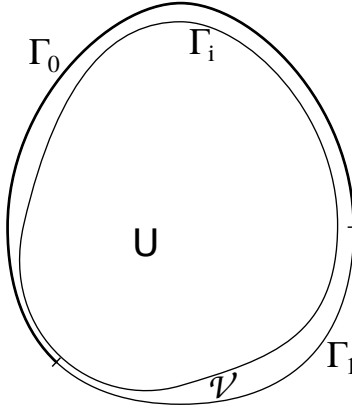


Figure 1: Example of a neighbourhood  $\mathcal{V}$ .

Since the boundary conditions are obviously satisfied on the accessible part  $\Gamma_0$ , we get  $(\mathbf{f}, \mathbf{g}) \in C(\varepsilon_1, \sigma_1; \Gamma_0)$  and thus  $(\mathbf{f}, \mathbf{g}) \in C(\varepsilon_2, \sigma_2; \Gamma_0) = C(\varepsilon_1, \sigma_1; \Gamma_0)$  by assumption. Therefore, there is a field  $\mathbf{E}_2 \in H(\mathbf{curl}; \Omega)$  such that

$$\begin{cases} \mathbf{curl} \mathbf{curl} \mathbf{E}_2 - k^2 \kappa_2 \mathbf{E}_2 &= 0, & \text{in } \Omega, \\ \mathbf{E}_2 \times \mathbf{n} = \mathbf{f}, & \text{on } \Gamma_0, \\ \mathbf{curl} \mathbf{E}_2 \times \mathbf{n} = \mathbf{g}, & \text{on } \Gamma_0, \end{cases} \quad (3)$$

where we emphasize that the boundary conditions are only satisfied on  $\Gamma_0$ .

The unique continuation principle (see [13, Lemma 5.4] which fits with the above regularity assumptions) applied to the difference  $\mathbf{E} = \mathbf{E}_1 - \mathbf{E}_2$  in the neighbourhood  $\mathcal{V}$  of  $\Gamma$  then yields  $\mathbf{E} = 0$  in  $\overline{\mathcal{V}}$  since

$$\begin{cases} \mathbf{curl} \mathbf{curl} \mathbf{E} - k^2 \kappa \mathbf{E} &= 0, & \text{in } \mathcal{V}, \\ \mathbf{E} \times \mathbf{n} = 0, & \text{on } \Gamma_0, \\ \mathbf{curl} \mathbf{E} \times \mathbf{n} = 0, & \text{on } \Gamma_0, \end{cases} \quad (4)$$

where  $\kappa = (\varepsilon_1 + i\sigma_1/\omega)/\varepsilon_0 = (\varepsilon_2 + i\sigma_2/\omega)/\varepsilon_0$  by assumption.

Consequently,  $\mathbf{E}_1 \times \mathbf{n} = \mathbf{E}_2 \times \mathbf{n} = \mathbf{f}$  and  $\mathbf{curl} \mathbf{E}_1 \times \mathbf{n} = \mathbf{curl} \mathbf{E}_2 \times \mathbf{n} = \mathbf{g}$  on the whole boundary  $\Gamma$  and  $(\mathbf{f}, \mathbf{g})$  belong to the Cauchy data set  $C(\varepsilon_2, \sigma_2; \Gamma)$ . Changing the roles of  $(\varepsilon_1, \sigma_1)$  and  $(\varepsilon_2, \sigma_2)$  proves that

$$C(\varepsilon_1, \sigma_1; \Gamma) = C(\varepsilon_2, \sigma_2; \Gamma). \quad (5)$$

Now, we infer from the assumptions on the coefficients that  $\partial^\alpha \varepsilon_1(\mathbf{x}) = \partial^\alpha \varepsilon_2(\mathbf{x})$  and  $\partial^\alpha \sigma_1(\mathbf{x}) = \partial^\alpha \sigma_2(\mathbf{x})$  for  $\alpha \in \mathbb{N}^3$  on the boundary  $\Gamma$  for any multi-index  $\alpha$  such that  $|\alpha| \leq 1$ . These properties are the assumptions of the global uniqueness Theorem of Caro and Zhou (see [17, Theorem 1.1]). This gives  $\varepsilon_1 = \varepsilon_2$  and  $\sigma_1 = \sigma_2$  in  $\Omega$  and completes the proof.  $\blacksquare$

Theorem 2.4 assumes that the electric permittivity  $\varepsilon$  and conductivity  $\sigma$  are known in a neighbourhood of  $\Gamma$ . Notice however, that no condition for the electric field is prescribed on the inaccessible part  $\Gamma_1$ . This hypothesis is less restrictive than geometrical or boundary conditions on  $\Gamma_1$ . Indeed, in the biomedical applications that we have in mind, the computational domain represents a head model, and the aim is to identify inner perturbations of a healthy background. In the neighbourhood of the head surface the electromagnetic coefficients can thus be fixed to known (constant) values available from the literature [30, 34], and the uniqueness theorem applies.

### 3 The quasi-reversibility method for Maxwell's equations

In view of the numerical resolution of the inverse coefficient problem in the domain  $\Omega$ , it is interesting to propose methods which are able to compute, in a stable way, the electric field  $\mathbf{E}$  on the domain  $\bar{\mathcal{V}}$  (see Figure 1) from known electric coefficients  $\varepsilon$  and  $\sigma$  (assumptions of Theorem 2.4) and partial boundary data, and then to solve the inverse problem in the remaining domain  $U = \Omega \setminus \bar{\mathcal{V}}$  from total data  $(\mathbf{E}|_{\Gamma_i} \times \mathbf{n}, \mathbf{curl} \mathbf{E}|_{\Gamma_i} \times \mathbf{n})$  on the interface  $\Gamma_i$  (see Figure 1). The aim is thus to map a couple of Cauchy data given on the accessible part  $\Gamma_0$ , onto the interior boundary of  $\partial\mathcal{V}$ , and this even if the data on  $\Gamma_0$  are corrupted by noise. This requires the resolution of a Cauchy problem in the domain  $\mathcal{V}$  which is known to be ill-posed.

The rest of the paper is devoted to the solution of this data completion problem for Maxwell's equations.

#### 3.1 Principle

The method of quasi-reversibility (called hereafter QR method) provides a regularized solution of Cauchy problems (which are known to be ill-posed) in a bounded domain. It has been introduced in [29] for elliptic equations and has been originally revisited in [28, 10]. In particular, Bourgeois proposed a mixed formulation of quasi-reversibility for Laplace's equation [10]. Here we adapt it to Maxwell's equations. The Cauchy problem reads: find  $\mathbf{E} \in H(\mathbf{curl}; \Omega)$  solution to

$$\begin{cases} \mathbf{curl} \mathbf{curl} \mathbf{E} - k^2 \kappa \mathbf{E} = 0, & \text{in } \Omega, \\ \mathbf{E} \times \mathbf{n} = \mathbf{f}, & \text{on } \Gamma_0, \\ \mathbf{curl} \mathbf{E} \times \mathbf{n} = \mathbf{g}, & \text{on } \Gamma_0. \end{cases} \quad (6)$$

Let us introduce the spaces  $V_{\mathbf{f}} = \{\mathbf{u} \in H(\mathbf{curl}; \Omega) ; \gamma_t(\mathbf{u}) = \mathbf{f} \text{ on } \Gamma_0\}$  for any  $\mathbf{f} \in Y(\Gamma_0)$  and  $M = \{\boldsymbol{\mu} \in H(\mathbf{curl}); \gamma_T(\boldsymbol{\mu}) = 0 \text{ on } \Gamma_1\}$ , where  $\gamma_T: H(\mathbf{curl}; \Omega) \rightarrow Y(\Gamma)'$  and  $\gamma_T(\boldsymbol{\mu}) = \mathbf{n} \times (\boldsymbol{\mu}|_{\Gamma} \times \mathbf{n})$  for smooth vector fields  $\boldsymbol{\mu}$  (see [26] for details). We may notice that fields in the vector space  $M$  satisfy  $\gamma_T(\boldsymbol{\mu}) = 0$  on the interior of  $\Gamma_1$ . Assume that  $(\mathbf{f}, \mathbf{g}) \in C(\varepsilon, \sigma; \Gamma_0)$  (see Definition 2.3) where  $\varepsilon$  and  $\sigma$  are admissible coefficients (see Definition 2.2). We denote by  $a(\cdot, \cdot)$  the sesqui-linear form corresponding to (1):  $a(\mathbf{u}, \mathbf{v}) = (\mathbf{curl} \mathbf{u}, \mathbf{curl} \mathbf{v}) - k^2(\kappa \mathbf{u}, \mathbf{v})$  with  $\mathbf{u}, \mathbf{v} \in H(\mathbf{curl}; \Omega)$  and  $(\cdot, \cdot)$  the dot-product in  $L^2$ . On  $H(\mathbf{curl}; \Omega)$ , we introduce the linear form  $\ell(\cdot)$  defined by  $\ell(\boldsymbol{\psi}) = \langle \mathbf{g}, \gamma_T(\boldsymbol{\psi}) \rangle_{Y(\Gamma_0), Y(\Gamma_0)'}$ . For small  $\delta > 0$ , we consider the following weak mixed formulation: Find  $(\mathbf{E}_\delta, \mathbf{F}_\delta) \in V_{\mathbf{f}} \times M$  such that

$$\begin{cases} \delta(\mathbf{E}_\delta, \boldsymbol{\phi})_{H(\mathbf{curl}; \Omega)} + a(\boldsymbol{\phi}, \mathbf{F}_\delta) = 0, & \forall \boldsymbol{\phi} \in V_0, \\ a(\mathbf{E}_\delta, \boldsymbol{\psi}) - (\mathbf{F}_\delta, \boldsymbol{\psi})_{H(\mathbf{curl}; \Omega)} = \ell(\boldsymbol{\psi}), & \forall \boldsymbol{\psi} \in M, \end{cases} \quad (7)$$

where  $(\cdot, \cdot)_{H(\mathbf{curl}; \Omega)}$  denotes the dot-product in  $H(\mathbf{curl}; \Omega)$ . Theorem 3.2 states that the regularized solution  $(\mathbf{E}_\delta, \mathbf{F}_\delta)$  tends to  $(\mathbf{E}, 0)$  solution to (6) when  $\delta$  tends to 0. The proof needs the following preliminary Lemma.

**Lemma 3.1.** *The partial trace application  $\mathbf{u} \mapsto \gamma_t(\mathbf{u})|_{\Gamma_0}$  is linear, continuous and surjective from  $H(\mathbf{curl}; \Omega)$  to  $Y(\Gamma_0)$ . Moreover, there exists a continuous lifting application: we can find a constant  $r > 0$  such that, for any  $\mathbf{v} \in Y(\Gamma_0)$ , there exists  $\mathbf{u} \in H(\mathbf{curl}; \Omega)$  with  $\gamma_t(\mathbf{u})|_{\Gamma_0} = \mathbf{v}$  and  $\|\mathbf{u}\|_{H(\mathbf{curl}; \Omega)} \leq r \|\mathbf{v}\|_{Y(\Gamma_0)}$ .*

Lemma 3.1 is a direct consequence of the fact that the trace application  $\gamma_t$  is linear, continuous and surjective from  $H(\mathbf{curl}; \Omega)$  to  $Y(\Gamma)$  (see [26]). Then, we build an homeomorphism between  $H(\mathbf{curl}; \Omega) / \mathcal{V}_0$  and  $Y(\Gamma_0)$ .

**Theorem 3.2.** *Let  $(\mathbf{f}, \mathbf{g}) \in Y(\Gamma_0) \times Y(\Gamma_0)$ . For any  $\delta > 0$ , problem (7) admits a unique solution  $(\mathbf{E}_\delta, \mathbf{F}_\delta) \in V_{\mathbf{f}} \times M$ .*

If, in addition,  $(\mathbf{f}, \mathbf{g})$  belongs to the Cauchy data set  $C(\varepsilon, \sigma; \Gamma_0)$ , then

$$\lim_{\delta \rightarrow 0} (\mathbf{E}_\delta, \mathbf{F}_\delta) = (\mathbf{E}, 0) \quad (8)$$

in  $V_f \times M$ . Here,  $\mathbf{E}$  is the unique solution in the set

$$K = \{\mathbf{v} \in V_f ; a(\mathbf{v}, \psi) = \ell(\psi) \quad \forall \psi \in M\}$$

of the minimization problem

$$\inf_{\mathbf{v} \in K} \|\mathbf{v}\|_{H(\mathbf{curl}; \Omega)}. \quad (9)$$

**Proof.** The proof relies on the arguments given in [12] where an abstract setting of the quasi-reversibility method is presented (see also [10]). Indeed, problem (7) can be written in closed form as a classical variational formulation in the unknowns  $(\mathbf{E}_\delta, \mathbf{F}_\delta)$ , involving a continuous and coercive sesqui-linear form  $A_\delta((\cdot, \cdot))$  defined on  $H(\mathbf{curl}; \Omega) \times M$ . Existence and uniqueness thus follow from Lax-Milgram's Lemma. In Section 4, we address convergence in a more general setting for a relaxed version of (7). Since the arguments are similar, we omit the convergence proof here and refer the reader to the proof of Theorem 4.1 for details. ■

## 3.2 Discretization by FEM and numerical results

The numerical solver for the 2D Maxwell equations has been implemented with FreeFem++ (see [24]). We consider a regular triangulation  $\mathcal{T}_h$  of  $\bar{\Omega}$ . For any  $T \in \mathcal{T}_h$ , let  $h_T$  be its diameter. Then  $h = \max_{T \in \mathcal{T}_h} h_T$  is the mesh parameter of  $\mathcal{T}_h$ . Edge finite elements of order 1 (see [31]) are used to approximate the solution of the regularized problem (7). Standard arguments in variational theory give an existence and uniqueness result for the associated discretized formulation of (7). Since problem (7) can be written as a variational formulation with a continuous and coercive sesqui-linear form, the discrete problem enters within the framework of C ea's lemma. The discretization error is thus proportional to the interpolation error which is of order  $\mathcal{O}(h)$  for the considered finite elements (see e.g. [26]) provided the continuous solution  $(\mathbf{E}_\delta, \mathbf{F}_\delta)$  is regular. However, the coercivity constant of the involved sesqui-linear form is given by  $\min\{\delta, 1\}$  and the discretization error thus behaves as  $\mathcal{O}(\frac{h}{\delta})$ . The regularization parameter  $\delta$  has thus to be chosen with respect to the mesh size and arbitrary small values of  $\delta$  are prohibited.

In all the simulations, we fix  $\varepsilon_0 = \mu_0 = \omega = 1$  and  $\kappa = 1 + i$ . Our reference solution is the plane wave  $\mathbf{E}(\mathbf{x}) = \boldsymbol{\eta}^\perp e^{ik\sqrt{\kappa}\boldsymbol{\eta} \cdot \mathbf{x}}$  where  $\boldsymbol{\eta} \in \mathbb{R}^2$  is the wave propagation vector and  $\boldsymbol{\eta}^\perp$  is a unit vector orthogonal to  $\boldsymbol{\eta}$ . The square-root  $\sqrt{\kappa}$  stands for the classical complex square-root with branch-cut along the negative real axis.

### 3.2.1 Unit disc

In the first example,  $\Omega$  is the unit disc discretized with a mesh of size  $h = 2.26\text{e-}2$ , ending up with 43 256 triangles and 65 134 edges. Two different configurations of accessible/inaccessible parts are tested (cf. Figure 2):

1. In the configuration G34,  $\Gamma_0$  is the arc of circle starting at angle 0 and ending at angle  $\frac{3\pi}{2}$ . The accessible part then represents 75% of the boundary  $\Gamma$ .
2. In the configuration GE37,  $\Gamma_0$  represents a set of 37 equally distributed electrodes of common length  $\frac{\pi}{25}$ . Electrodes cover 81.6% of the boundary  $\Gamma$ .

In Figure 3, we show the relative error in the  $L^2(\Omega)$ -norm between the exact solution  $\mathbf{E}$  and its approximation obtained by the numerical resolution of (7), with respect to  $\delta$ . For both configurations, we indicate the parameter  $\delta$  for which the error is minimal. Notice that the behaviour of the error for

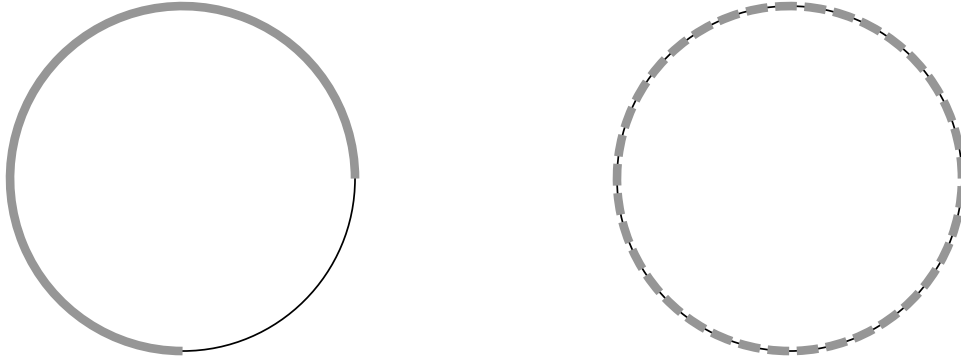


Figure 2: Choice of the accessible part  $\Gamma_0$  (grey line). Left: configuration G34. Right: configuration GE37.

the configuration G34 shown in Figure 3 is in agreement with the error analysis which claims that the error behaves as  $\mathcal{O}(\frac{h}{\delta})$ : at fixed mesh size the error increases for small values of  $\delta$ .

In Table 1, we report different errors obtained for the value  $\delta = 9.103 \cdot 10^{-7}$ . The approximation of the electric field  $\mathbf{E}$  is more accurate on the whole domain  $\Omega$  than on the inaccessible part  $\Gamma_1$ . The configuration GE37 yields better results since the accessible part covers a larger part of the boundary  $\Gamma$ . In Figure 4, we illustrate these results by plotting the modulus of the error  $|\mathbf{E} - \mathbf{E}_\delta|$  in the domain  $\Omega$ . The largest errors are located on  $\Gamma_1$ , and in particular at the intersection between  $\Gamma_0$  and  $\Gamma_1$ .

Indeed, the solution  $(\mathbf{E}_\delta, \mathbf{F}_\delta)$  of (7) is the weak solution of a boundary value problem in  $\Omega$  with mixed boundary conditions for  $\mathbf{E}_\delta$  and  $\mathbf{F}_\delta$ . Mixed boundary conditions are known to induce singularities in the fields unless the data do not satisfy some compatibility conditions (see e.g. [23] for the simpler case of the Laplace operator). In the present case, it is not clear whether these compatibility conditions are satisfied or not. This could explain the singular behavior at the intersection points.

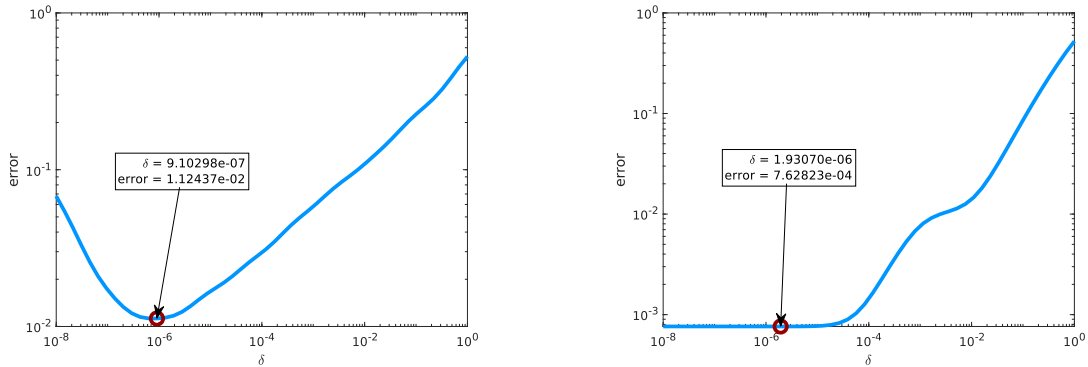


Figure 3: Unit disc. QR method. Relative error  $\frac{\|\mathbf{E} - \mathbf{E}_\delta\|_{0,\Omega}}{\|\mathbf{E}\|_{0,\Omega}}$  with respect to the regularization parameter  $\delta$ . Left: configuration G34. Right: configuration GE37.

### 3.2.2 Ring

For the inverse problem we are studying, we are interested in ring-like domains which, for instance, model the different tissues of the head. The goal consists in mapping the data measured on part of the exterior boundary to an inner interface, allowing in a second step to use reconstruction methods in the interior domain. In this section, we present numerical results on a ring of internal radius 0.75,

Table 1: Unit disc. QR method. Errors for  $\delta = 9.103 \cdot 10^{-7}$ .

Configuration	$\frac{\ \mathbf{E} - \mathbf{E}_\delta\ _{0,\Omega}}{\ \mathbf{E}\ _{0,\Omega}}$	$\frac{\ (\mathbf{E} - \mathbf{E}_\delta) \times \mathbf{n}\ _{0,\Gamma_1}}{\ \mathbf{E} \times \mathbf{n}\ _{0,\Gamma_1}}$	$\ \mathbf{F}_\delta\ _{0,\Omega}$
G34	1.1244e-02	1.7302e-01	1.8374e-04
GE37	7.6288e-04	1.5185e-02	1.8224e-04

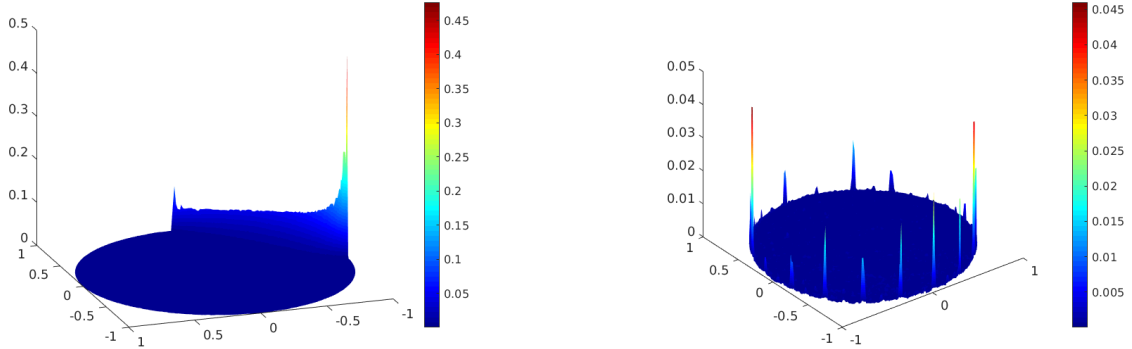


Figure 4: Unit disc. QR method. Modulus of the error  $|\mathbf{E} - \mathbf{E}_\delta|$ . Left: configuration G34. Right: configuration GE37.

discretized with a mesh size  $h = 2.05e-2$ , 17919 triangles and 27316 edges. Three measurement configurations are compared: G34 and GE37, both described in the previous section, and GExt where  $\Gamma_0$  is the whole external boundary (see Figure 5).

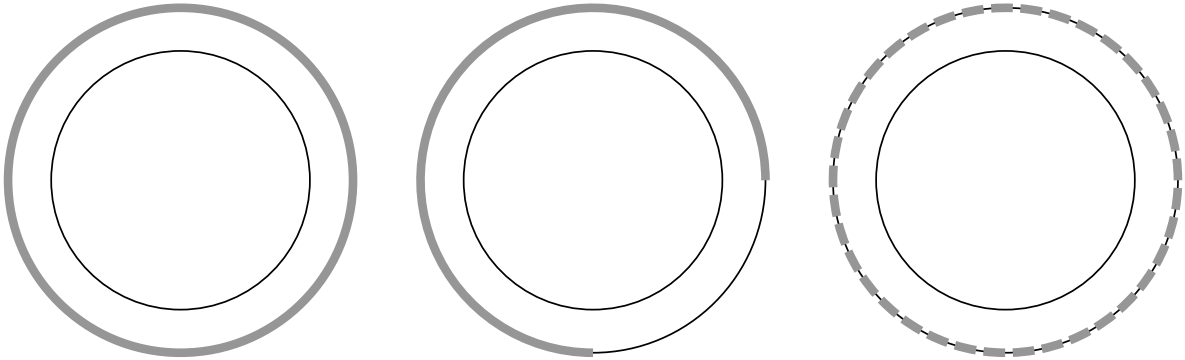


Figure 5: Choice of the accessible part  $\Gamma_0$  (grey line). Left: configuration GExt ( $\Gamma_0$  covers 57% of the ring boundary). Middle: configuration G34 (43%). Right: configuration GE37 (47%).

The relative errors with respect to  $\delta$  are shown in Figure 6. For each configuration, we list in Table 2 different errors obtained for the value  $\delta$  realizing the minimum indicated in Figure 6. Notice that we split the inaccessible part into an exterior part  $\Gamma_1$  and the interior circle  $\Gamma_i$ . Furthermore, the modulus of the error  $|\mathbf{E} - \mathbf{E}_\delta|$  is reported in Figure 7. We observe that the electric field  $\mathbf{E}$  is well approximated in the ring by the quasi-reversibility approach when the data are available on the entire exterior boundary (configuration GExt). The transmission of the information on the inner boundary  $\Gamma_i$  is very accurate. The configuration GE37 with electrodes leads also to very interesting results with errors below 4% on the inaccessible part  $\Gamma_1$  and the inner boundary  $\Gamma_i$ . The analysis of the results

obtained with configuration G34 is less obvious: whereas the error of the auxiliary field  $\mathbf{F}_\delta$  is very satisfying, we observe on  $\Omega$ ,  $\Gamma_1$  and  $\Gamma_i$  errors of 35 %, 70 %, and 48 %, respectively. The next section will propose a possible improvement of the quasi-reversibility method for such a configuration.

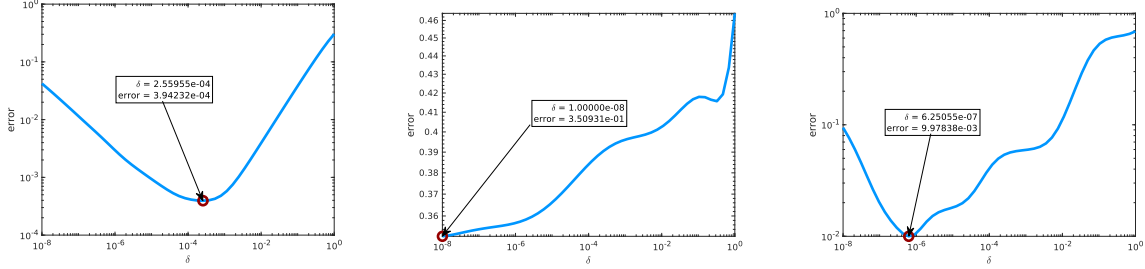


Figure 6: Ring. QR method. Relative error  $\frac{\|\mathbf{E} - \mathbf{E}_\delta\|_{0,\Omega}}{\|\mathbf{E}\|_{0,\Omega}}$  with respect to the regularization parameter  $\delta$ . Left: configuration GExt. Middle: configuration G34. Right: configuration GE37.

Table 2: Ring. QR method. Errors.

Configuration	$\frac{\ \mathbf{E} - \mathbf{E}_\delta\ _{0,\Omega}}{\ \mathbf{E}\ _{0,\Omega}}$	$\frac{\ (\mathbf{E} - \mathbf{E}_\delta) \times \mathbf{n}\ _{0,\Gamma_1}}{\ \mathbf{E} \times \mathbf{n}\ _{0,\Gamma_1}}$	$\frac{\ (\mathbf{E} - \mathbf{E}_\delta) \times \mathbf{n}\ _{0,\Gamma_i}}{\ \mathbf{E} \times \mathbf{n}\ _{0,\Gamma_i}}$	$\ \mathbf{F}_\delta\ _{0,\Omega}$
GExt	3.9423e-04	6.6661e-04	6.6661e-04	1.7964e-04
G34	3.5093e-01	6.9598e-01	4.8011e-01	8.1894e-05
GE37	9.9784e-03	3.9068e-02	3.8737e-02	8.4337e-05

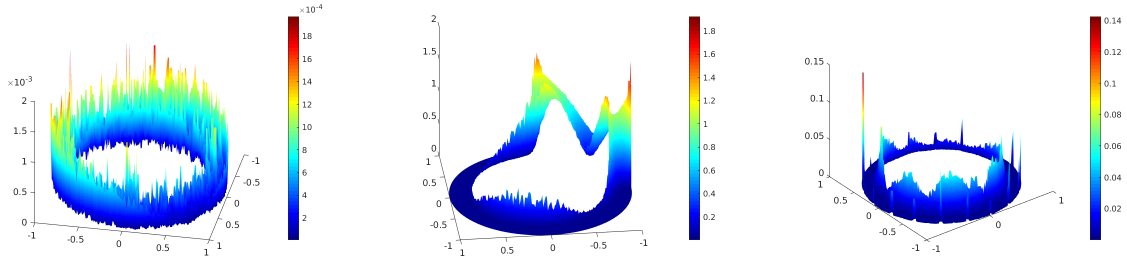


Figure 7: Ring. QR method. Modulus of the error  $|\mathbf{E} - \mathbf{E}_\delta|$ . Left: configuration GExt. Middle: configuration G34. Right: configuration GE37.

### 3.2.3 Extension of the computational domain

For similar configurations of the accessible part, the errors obtained on the disc are more accurate than on the ring. This leads us to the idea of extending the computational domain to a full disc  $\tilde{\Omega} = (\bar{\Omega} \cup \bar{\Omega}_{\text{int}})^\circ$  before restricting the solution to the initial ring  $\Omega$  through the Algorithm 1.

From a theoretical point of view, if the data  $(\mathbf{f}, \mathbf{g})$  belong to the Cauchy data set  $C(\tilde{\varepsilon}, \tilde{\sigma}; \Gamma_0)$  with respect to the extended domain  $\tilde{\Omega}$ , the sequence  $(\mathbf{E}_\delta, \tilde{\mathbf{F}}_\delta)$  converges to  $(\tilde{\mathbf{E}}, 0)$  where  $\tilde{\mathbf{E}}$  is the solution of the minimization problem (9) in  $\tilde{\Omega}$ . The restriction  $\mathbf{E}$  to the ring  $\Omega$  satisfies the Cauchy problem with data  $(\mathbf{f}, \mathbf{g})$  on  $\Omega$ . Thanks to the unique continuation principle,  $\mathbf{E}$  is the only possible solution and coincides with the limit of the sequence obtained by the quasi-reversibility method applied on  $\Omega$ .

Figure 8 shows the error with respect to  $\delta$  obtained by the extension/restriction method for the previous three configurations. The errors obtained with the values of  $\delta$  realizing the minima are reported

---

**Algorithm 1:** Extension/restriction method
 

---

**Input data:**  $(\mathbf{f}, \mathbf{g})$  on  $\Gamma_0$

extend the coefficients  $\varepsilon$  and  $\sigma$  defined on  $\Omega$  to admissible coefficients  $\tilde{\varepsilon}$  and  $\tilde{\sigma}$  defined on  $\tilde{\Omega}$ .

compute  $(\tilde{\mathbf{E}}_\delta, \tilde{\mathbf{F}}_\delta)$  on  $\tilde{\Omega}$  by the quasi-reversibility method.

define the final fields  $(\mathbf{E}_\delta, \mathbf{F}_\delta)$  by restriction of  $(\tilde{\mathbf{E}}_\delta, \tilde{\mathbf{F}}_\delta)$  to the ring  $\Omega$ .

---

in Table 3 and illustrated in Figure 9. We notice a significant improvement of the approximation on the inaccessible part: 12.5% instead of 70% on  $\Gamma_1$ , 0.8% instead of 48% on  $\Gamma_i$ . The drawback lies in the increasing computational cost since the extended domain leads to a larger number of unknowns.

The numerical results of the previous sections attest the efficiency of the quasi-reversibility method for Maxwell equations in the case of compatible data belonging to the trace space.

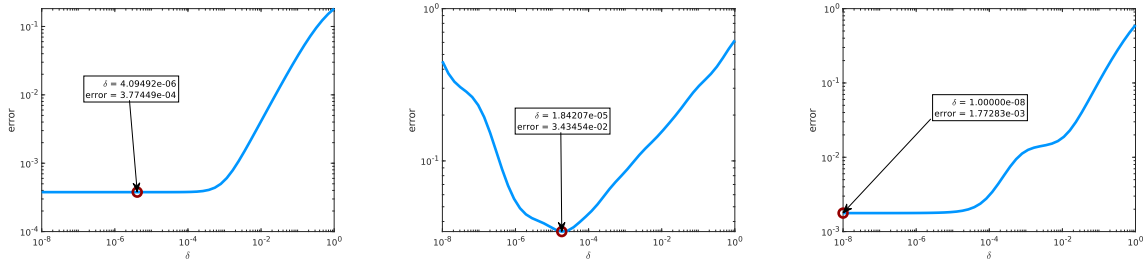


Figure 8: Ring. QR method. Extension/restriction method. Relative error  $\frac{\|\mathbf{E} - \mathbf{E}_\delta\|_{0,\Omega}}{\|\mathbf{E}\|_{0,\Omega}}$  with respect to the regularization parameter  $\delta$ . Left: configuration GExt. Middle: configuration G34. Right: configuration GE37.

Table 3: Ring. QR method. Extension/restriction method. Errors.

Configuration	$\frac{\ \mathbf{E} - \mathbf{E}_\delta\ _{0,\Omega}}{\ \mathbf{E}\ _{0,\Omega}}$	$\frac{\ (\mathbf{E} - \mathbf{E}_\delta) \times \mathbf{n}\ _{0,\Gamma_1}}{\ \mathbf{E} \times \mathbf{n}\ _{0,\Gamma_1}}$	$\frac{\ (\mathbf{E} - \mathbf{E}_\delta) \times \mathbf{n}\ _{0,\Gamma_i}}{\ \mathbf{E} \times \mathbf{n}\ _{0,\Gamma_i}}$	$\ \mathbf{F}_\delta\ _{0,\Omega}$
GExt	3.7745e-04	1.5665e-04	1.5665e-04	3.1125e-04
G34	3.4345e-02	1.2558e-01	8.1477e-03	2.6564e-04
GE37	1.7728e-03	1.1968e-02	2.9520e-04	9.0131e-05

## 4 A regularized relaxed mixed formulation

As pointed out in [12], noisy data will, in general, not belong to the trace space  $Y(\Gamma_0)$ . To overcome this difficulty, a relaxed version of the mixed problem (7) has been proposed. In this section, we follow a similar idea. However, the nature of the trace space which is a proper subspace of  $H^{-1/2}(\Gamma)$ , leads to a modification of the basic vector space. To this end, we will assume in the sequel that the boundary data  $(\mathbf{f}, \mathbf{g})$  belong to  $L^2(\Gamma_0)^3 \times L^2(\Gamma_0)^3$ . Notice that this assumption does not imply that the data belong to the trace space.

### 4.1 A first version

Consider the vector space

$$V = \{\mathbf{v} \in H(\mathbf{curl}; \Omega) ; \gamma_t(\mathbf{v}) \in L^2(\Gamma_0)^3\} \quad (10)$$

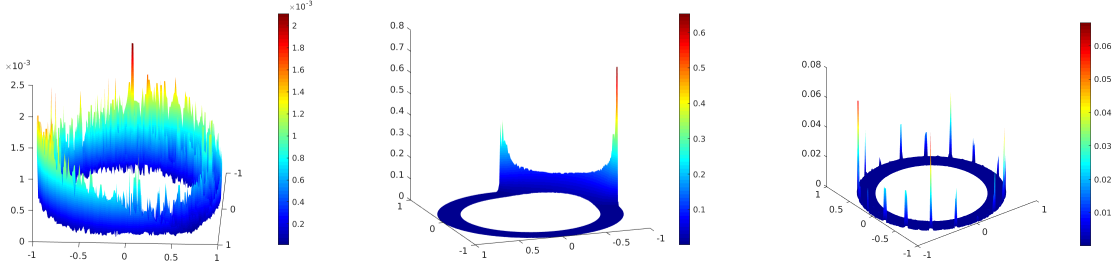


Figure 9: Ring. QR method. Extension/restriction method. Modulus of the error  $|\mathbf{E} - \mathbf{E}_\delta|$ . Left: configuration GExt. Middle: configuration G34. Right: configuration GE37.

with the norm

$$\|\mathbf{v}\|_V = \left( \|\mathbf{v}\|_{H(\mathbf{curl}; \Omega)}^2 + \|\gamma_t \mathbf{v}\|_{0, \Gamma_0}^2 \right)^{1/2}. \quad (11)$$

The space  $M$  will now be defined as the following subspace of  $V$ ,

$$M = \{\mathbf{v} \in V ; \gamma_T(\mathbf{v}) = 0 \text{ on } \Gamma_1\}, \quad (12)$$

equipped with the norm of  $V$ ,  $\|\cdot\|_V$ . Since we cannot assume that there is a lifting of the boundary data  $\mathbf{f}$  in  $V$ , the boundary condition will be imposed weakly through a penalization term. The relaxed version of the mixed problem then reads

$$\begin{cases} \text{Find } (\mathbf{E}_\alpha, \mathbf{F}_\alpha) \in V \times M \text{ such that} \\ \delta(\mathbf{E}_\alpha, \phi)_V + \eta^2(\gamma_t \mathbf{E}_\alpha, \gamma_t \phi)_{0, \Gamma_0} \\ \quad + a(\phi, \mathbf{F}_\alpha) = \eta^2(\mathbf{f}, \gamma_t \phi)_{0, \Gamma_0}, & \forall \phi \in V, \\ a(\mathbf{E}_\alpha, \psi) - (\mathbf{F}_\alpha, \psi)_V = \ell(\psi), & \forall \psi \in M, \end{cases} \quad (13)$$

where the subscript  $\alpha = (\delta, \eta)$  indicates that the solution of (13) depends on the regularization parameter  $\delta > 0$  and the relaxation parameter  $\eta > 0$ .

**Theorem 4.1.** *Let  $(\mathbf{f}, \mathbf{g}) \in L^2(\Gamma_0) \times L^2(\Gamma_0)$ . For any  $\alpha = (\delta, \eta)$  such that  $\delta > 0$  and  $\eta > 0$ , problem (13) admits a unique solution  $(\mathbf{E}_\alpha, \mathbf{F}_\alpha) \in V \times M$ .*

*If, in addition,  $(\mathbf{f}, \mathbf{g})$  belongs to the Cauchy data set  $C(\varepsilon, \sigma; \Gamma_0)$ , then*

$$\lim_{\delta \rightarrow 0} (\mathbf{E}_\alpha, \mathbf{F}_\alpha) = (\mathbf{E}, 0) \quad (14)$$

*in  $V \times M$  for any fixed  $\eta > 0$ . Here,  $\mathbf{E}$  is the unique solution in the set*

$$K_{\mathbf{f}} = \{\mathbf{v} \in V ; \gamma_t \mathbf{v} = \mathbf{f} \text{ on } \Gamma_0 \text{ and } a(\mathbf{v}, \psi) = \ell(\psi) \forall \psi \in M\}$$

*of the minimization problem*

$$\inf_{\mathbf{v} \in K_{\mathbf{f}}} \|\mathbf{v}\|_V. \quad (15)$$

*The following estimates hold true*

$$\|\mathbf{F}_\alpha\|_V \leq \sqrt{2\delta} \|\mathbf{E}\|_V \quad \forall \eta > 0, \quad (16)$$

$$\|\gamma_t \mathbf{E}_\alpha - \mathbf{f}\|_{0, \Gamma_0} \leq \frac{\sqrt{2\delta}}{\eta} \|\mathbf{E}\|_V. \quad (17)$$

The proof is based on ideas from [12] where the convergence result has been proven for the classical version. In addition, we prove here that a careful analysis of the arguments allows to obtain the

estimates (16) and (17). This gives further insight in the behavior of the sequence  $(\mathbf{E}_\alpha, \mathbf{F}_\alpha)$ . Indeed, (16) yields a convergence order for the convergence of  $\mathbf{F}_\alpha$  to 0 independently from the choice of  $\eta$ . Estimate (17) suggests that we should choose  $\eta$  such that  $\frac{\sqrt{2\delta}}{\eta} \rightarrow 0$ . Large values of  $\eta$  should accelerate the convergence of the trace of  $\mathbf{E}_\alpha$  on  $\Gamma_0$ .

**Proof.** Problem (13) can be written in the following closed form,

$$\begin{cases} \text{Find } (\mathbf{E}_\alpha, \mathbf{F}_\alpha) \in V \times M \text{ such that} \\ A_\alpha((\mathbf{E}_\alpha, \mathbf{F}_\alpha), (\phi, \psi)) = L_\alpha((\phi, \psi)) \quad \forall (\phi, \psi) \in V \times M, \end{cases}$$

where the sesqui-linear form  $A_\alpha(\cdot, \cdot)$  and the linear form  $L_\alpha(\cdot)$  are defined on  $V \times M$  by

$$A_\alpha((\mathbf{u}, \mathbf{v}), (\phi, \psi)) = \delta(\mathbf{u}, \phi)_V + \eta^2(\gamma_t \mathbf{u}, \gamma_t \phi)_{0, \Gamma_0} + a(\phi, \mathbf{v}) - a(\mathbf{u}, \psi) + (\mathbf{v}, \psi)_M$$

and

$$L_\alpha((\phi, \psi)) = \eta^2(\mathbf{f}, \gamma_t \phi)_{0, \Gamma_0} - \ell(\psi).$$

The continuity of  $A_\alpha(\cdot, \cdot)$  and  $L_\alpha(\cdot)$  is obvious, and coercivity follows since

$$A_\alpha((\mathbf{u}, \mathbf{v}), (\mathbf{u}, \mathbf{v})) = \delta \|\mathbf{u}\|_V^2 + \eta^2 \|\gamma_t \mathbf{u}\|_{0, \Gamma_0}^2 + \|\mathbf{v}\|_V^2 \geq \min(\delta, 1) \|(\mathbf{u}, \mathbf{v})\|_{V \times V}^2$$

taking into account that the scalar product in  $M$  is the one of  $V$ . We thus can apply Lax-Milgram's Lemma to prove existence and uniqueness of a solution of problem (13).

Now consider the minimization problem (15) on  $K_{\mathbf{f}}$ . According to the assumption  $(\mathbf{f}, \mathbf{g}) \in C(\varepsilon, \sigma; \omega)$ , the set  $K_{\mathbf{f}}$  is not empty. It is obviously convex. The strictly convex functional  $\mathbf{v} \mapsto \|\mathbf{v}\|_V$  thus admits a unique minimum  $\mathbf{E}$  satisfying  $\gamma_t \mathbf{E} = \mathbf{f}$  and

$$a(\mathbf{E}, \psi) = \ell(\psi) \quad \forall \psi \in M.$$

Together with the second equation of problem (13), we get

$$a(\mathbf{E}_\alpha - \mathbf{E}, \psi) - (\mathbf{F}_\alpha, \psi)_V = 0 \quad \forall \psi \in M. \quad (18)$$

Now, take  $\phi = \mathbf{E}_\alpha - \mathbf{E}$  in problem (13) and  $\psi = \mathbf{F}_\alpha$  in (18) and subtract the latter from the first one. Taking into account that  $\gamma_t \mathbf{E} = \mathbf{f}$ , this yields the fundamental relation

$$\delta(\mathbf{E}_\alpha, \mathbf{E}_\alpha - \mathbf{E})_V + \eta^2 \|\gamma_t \mathbf{E}_\alpha - \mathbf{f}\|_{0, \Gamma_0}^2 + \|\mathbf{F}_\alpha\|_V^2 = 0. \quad (19)$$

From (19), we see that  $\|\mathbf{E}_\alpha\|_V \leq \|\mathbf{E}\|_V$ , i.e. the sequence  $(\mathbf{E}_\alpha)_\alpha$  is bounded with respect to the two parameters  $\delta$  and  $\eta$ . We then deduce from (19) estimation (16),

$$\|\mathbf{F}_\alpha\|_V \leq \sqrt{2\delta} \|\mathbf{E}\|_V,$$

and thus the convergence of  $(\mathbf{F}_\alpha)_\alpha$  to 0 whenever the regularization parameter  $\delta$  tends to 0.

The boundary term can be estimated in a similar way,

$$\|\gamma_t \mathbf{E}_\alpha - \mathbf{f}\|_{0, \Gamma_0} \leq \frac{\sqrt{2\delta}}{\eta} \|\mathbf{E}\|_V,$$

which yields estimation (17). In particular, the sequence  $(\gamma_t \mathbf{E}_\alpha)_\alpha$  tends to  $\mathbf{f}$  if  $\lim_{\delta \rightarrow 0} \left( \frac{\sqrt{2\delta}}{\eta} \right) = 0$  which is, for example, the case for any fixed  $\eta > 0$ .

It remains to prove the convergence of the sequence  $(\mathbf{E}_\alpha)_\alpha$ . Recall that the sequence is bounded in  $V$  which is a Hilbert space. Therefore, there is a subsequence of  $(\mathbf{E}_\alpha)_\alpha$  that converges weakly in  $V$  to a limit field  $\tilde{\mathbf{E}}$ .

Passing to the limit in the second equation of (13) yields

$$a(\tilde{\mathbf{E}}, \boldsymbol{\psi}) = \ell(\boldsymbol{\psi}) \quad \forall \boldsymbol{\psi} \in M$$

if  $\delta \rightarrow 0$ . Moreover, we get on the one hand

$$(\gamma_t \mathbf{E}_\alpha, \boldsymbol{\xi})_{0, \Gamma_0} \rightarrow (\gamma_t \tilde{\mathbf{E}}, \boldsymbol{\xi})_{0, \Gamma_0} \quad \forall \boldsymbol{\xi} \in L^2(\Gamma_0)^3, \quad \boldsymbol{\xi} \cdot \mathbf{n} = 0 \text{ on } \Gamma_0$$

from the weak convergence of  $(\mathbf{E}_\alpha)_\alpha$  in  $V$  and the density of  $Y(\Gamma_0) \cap L^2(\Gamma_0)^3$  in the subspace of tangential fields of  $L^2(\Gamma_0)^3$ , and on the other

$$\gamma_t \mathbf{E}_\alpha \rightarrow \mathbf{f}$$

strongly in  $L^2(\Gamma_0)^3$  according to (17) and the assumptions on the parameter set  $\alpha$ . Consequently, the limit field  $\tilde{\mathbf{E}}$  satisfies  $\gamma_t \tilde{\mathbf{E}} = \mathbf{f}$  and thus belongs to the set  $K_f$ . The uniqueness of the solution to the minimization problem thus yields  $\tilde{\mathbf{E}} = \mathbf{E}$ .

Then,

$$\begin{aligned} \|\mathbf{E}_\alpha - \mathbf{E}\|_V^2 &= \mathcal{R}((\mathbf{E}_\alpha, \mathbf{E}_\alpha - \mathbf{E})_V - (\mathbf{E}, \mathbf{E}_\alpha - \mathbf{E})_V) \\ &= -\frac{\eta^2}{\delta} \|\gamma_t(\mathbf{E}_\alpha - \mathbf{E})\|_{0, \Gamma_0}^2 - \frac{1}{\delta} \|\mathbf{F}_\alpha\|_V^2 - \mathcal{R}((\mathbf{E}, \mathbf{E}_\alpha - \mathbf{E})) \\ &\leq -\mathcal{R}((\mathbf{E}, \mathbf{E}_\alpha)) + \|\mathbf{E}\|_V^2. \end{aligned}$$

Since  $(\mathbf{E}_\alpha)_\alpha$  converges weakly to  $\mathbf{E}$ , the above inequality implies the strong convergence, at least for a subsequence. It follows from a standard argument that the whole sequence converges strongly to  $\mathbf{E}$  which completes the proof.  $\blacksquare$

## 4.2 A second version

The choice of the space  $V$  in the preceding section has been motivated by the penalization of the boundary condition  $\mathbf{E} \times \mathbf{n} = \mathbf{f}$  which can no longer be imposed strongly if the data do not belong to the trace space  $Y(\Gamma_0)$ . One may ask however if it is judicious to restrict the belonging of the fields trace to  $L^2$  on the accessible part  $\Gamma_0$  only. It seems thus natural to investigate another choice for the basic vector space: let

$$W := \{\mathbf{v} \in H(\mathbf{curl}; \Omega); \gamma_t(\mathbf{v}) \in L^2(\Gamma)^3\} \quad (20)$$

with the norm

$$\|\mathbf{v}\|_W = \left( \|\mathbf{v}\|_{H(\mathbf{curl}; \Omega)}^2 + \|\gamma_t \mathbf{v}\|_{0, \Gamma}^2 \right)^{1/2}. \quad (21)$$

Notice that the space  $M$  defined in (12) keeps unchanged since the boundary condition  $\mathbf{v} \times \mathbf{n} = 0$  on  $\Gamma_1$  implies, together with the condition  $\mathbf{v} \in V$  that  $M \subset W$  and  $\|\mathbf{v}\|_V = \|\mathbf{v}\|_W$  for any field in  $M$ .

In order to obtain the associated relaxed formulation, we have several choices. We obviously could just replace the space  $V$  by  $W$  in the formulation of problem in (13). The existence and uniqueness of a solution to the mixed problem on  $W$  can be proved in the same way as in the proof of Theorem 4.1. A slight modification occurs in the proof of the convergence of the sequence  $(\mathbf{E}_\alpha, \mathbf{F}_\alpha)$ . Indeed, this requires that the Cauchy problem (6) admits a solution in the modified vector space  $W$  and implies more regularity of the limit field  $\mathbf{E}$  on  $\Gamma_1$ . The rest of the proof keeps unchanged.

From a numerical point of view, it seems however appealing to introduce a new parameter  $\nu > 0$  that acts as a regularization parameter on the inaccessible part  $\Gamma_1$  of the boundary. An appropriate "tuning" of the parameters should allow to improve the numerical results.

In view of the latter remark, we define the relaxed mixed problem with regularization on  $\Gamma_1$  as follows:

$$\left\{ \begin{array}{l} \text{Find } (\mathbf{E}_\beta, \mathbf{F}_\beta) \in W \times M \text{ such that} \\ \delta(\mathbf{E}_\beta, \boldsymbol{\phi})_V + \nu(\gamma_t \mathbf{E}_\beta, \gamma_t \boldsymbol{\phi})_{0, \Gamma_1} \\ \quad + \eta^2(\gamma_t \mathbf{E}_\beta, \gamma_t \boldsymbol{\phi})_{0, \Gamma_0} + a(\boldsymbol{\phi}, \mathbf{F}_\beta) = \eta^2(\mathbf{f}, \gamma_t \boldsymbol{\phi})_{0, \Gamma_0}, \quad \forall \boldsymbol{\phi} \in W, \\ \quad a(\mathbf{E}_\beta, \boldsymbol{\psi}) - (\mathbf{F}_\beta, \boldsymbol{\psi})_W = \ell(\boldsymbol{\psi}), \quad \forall \boldsymbol{\psi} \in M, \end{array} \right. \quad (22)$$

where the subscript  $\beta = (\delta, \nu, \eta)$  indicates that the solution of (13) depends on the regularization parameters  $\delta > 0$  and  $\nu > 0$  as well as on the relaxation parameter  $\eta > 0$ .

Notice that the first two terms in the first equation are well defined according to the definition of the space  $W$ , but that the weight of the different parts of the norm can be chosen independently.

**Theorem 4.2.** *Let  $(\mathbf{f}, \mathbf{g}) \in L^2(\Gamma_0)^3 \times L^2(\Gamma_0)^3$ . For any  $\beta = (\delta, \nu, \eta)$  such that  $\delta > 0$ ,  $\nu > 0$  and  $\eta > 0$ , problem (22) admits a unique solution  $(\mathbf{E}_\beta, \mathbf{F}_\beta) \in W \times M$ .*

*If, in addition,  $(\mathbf{f}, \mathbf{g})$  belongs to the Cauchy data set  $C(\varepsilon, \sigma; \omega)$  such that there is a solution of the Cauchy problem (6) in the space  $W$ , then for any fixed  $\eta > 0$ ,*

$$\lim_{(\delta, \nu) \rightarrow 0} (\mathbf{E}_\beta, \mathbf{F}_\beta) = (\mathbf{E}, 0) \quad (23)$$

in  $W \times M$  whenever the parameters  $\delta$  and  $\nu$  satisfy the relation

$$\lim_{(\delta, \nu) \rightarrow 0} \frac{\delta}{\nu} = 1. \quad (24)$$

Here,  $\mathbf{E}$  is the unique solution in the set

$$K_f = \{\mathbf{v} \in W ; \gamma_t \mathbf{v} = \mathbf{f} \text{ on } \Gamma_0 \text{ and } a(\mathbf{v}, \boldsymbol{\psi}) = \ell(\boldsymbol{\psi}) \ \forall \boldsymbol{\psi} \in M\}$$

of the minimization problem

$$\inf_{\mathbf{v} \in K_f} \|\mathbf{v}\|_W. \quad (25)$$

The proof is similar to the one of Theorem 4.1 and we only point out the influence of the parameter  $\nu$  on the different steps of the proof.

**Proof.** As before, problem (22) can be written in variational form involving a continuous and coercive sesqui-linear form on  $W \times M$ . The coercivity constant is now given by  $\min(\delta, \nu)$ .

The assumptions guarantee that the set  $K_f$  is not empty and the minimization problem (25) admits a unique solution  $\mathbf{E}$ .

The orthogonality relation now reads as follows,

$$\delta(\mathbf{E}_\beta, \mathbf{E}_\beta - \mathbf{E})_V + \nu(\gamma_t \mathbf{E}_\beta, \gamma_t(\mathbf{E}_\beta - \mathbf{E}))_{0, \Gamma_1} + \eta^2 \|\gamma_t \mathbf{E}_\beta - \mathbf{f}\|_{0, \Gamma_0}^2 + \|\mathbf{F}_\beta\|_W^2 = 0. \quad (26)$$

Developping the scalar products and applying Cauchy-Schwarz' inequality on the real parts yields the following estimation of  $(\mathbf{E}_\beta)$

$$\delta \|\mathbf{E}_\beta\|_V^2 + \nu \|\gamma_t \mathbf{E}_\beta\|_{0, \Gamma_1}^2 \leq \delta \|\mathbf{E}_\beta\|_V \|\mathbf{E}\|_V + \nu \|\gamma_t \mathbf{E}_\beta\|_{0, \Gamma_1} \|\gamma_t \mathbf{E}\|_{0, \Gamma_1}.$$

In order to get estimates for the  $W$ -norm, we notice that the left hand side can be minored by  $\min(\delta, \nu) \|\mathbf{E}_\beta\|_W^2$ , whereas the right hand side can be majored by  $\max(\delta, \nu) \|\mathbf{E}_\beta\|_W \|\mathbf{E}\|_W$ . Consequently,

$$\|\mathbf{E}_\beta\|_W \leq \frac{\max(\delta, \nu)}{\min(\delta, \nu)} \|\mathbf{E}\|_W. \quad (27)$$

Under the given assumptions, the sequence  $(\mathbf{E}_\beta)_\beta$  is thus bounded in  $W$  and we obtain as before that  $\mathbf{F}_\beta$  converges to 0 in  $M$  when  $(\delta, \nu) \rightarrow 0$  since

$$\begin{aligned} \|\mathbf{F}_\beta\|_W^2 &\leq \delta \|\mathbf{E}_\beta\|_V \|\mathbf{E}_\beta - \mathbf{E}\|_V + \nu \|\gamma_t \mathbf{E}_\beta\|_{0, \Gamma_1} \|\gamma_t(\mathbf{E}_\beta - \mathbf{E})\|_{0, \Gamma_1} \\ &\leq \frac{1}{2} \max(\delta, \nu) \|\mathbf{E}_\beta\|_W \|\mathbf{E}_\beta - \mathbf{E}\|_W \\ &\leq \max(\delta, \nu) \|\mathbf{E}\|_W^2. \end{aligned}$$

In the same way, we get

$$\|\gamma_t \mathbf{E}_\beta - \mathbf{f}\|_{0,\Gamma_0} \leq \frac{\sqrt{\max(\delta, \nu)}}{\eta} \|\mathbf{E}\|_W.$$

As before, we prove that the sequence  $(\mathbf{E}_\beta)_\beta$  converges weakly to the solution  $\mathbf{E}$  of the minimization problem. In order to show strong convergence, we notice that, according to (26),

$$\delta \mathcal{R}((\mathbf{E}_\beta, \mathbf{E}_\beta - \mathbf{E})_V) + \nu \mathcal{R}((\gamma_t \mathbf{E}_\beta, \gamma_t (\mathbf{E}_\beta - \mathbf{E}))_{0,\Gamma_1}) \leq 0.$$

Hence,

$$\begin{aligned} \|\mathbf{E}_\beta - \mathbf{E}\|_W^2 &= \mathcal{R}((\mathbf{E}_\beta, \mathbf{E}_\beta - \mathbf{E})_W) - \mathcal{R}((\mathbf{E}, \mathbf{E}_\beta - \mathbf{E})_W) \\ &\leq \left(1 - \frac{\delta}{\nu}\right) \mathcal{R}((\mathbf{E}_\beta, \mathbf{E}_\beta - \mathbf{E})_V) - \mathcal{R}((\mathbf{E}, \mathbf{E}_\beta - \mathbf{E})_W) \\ &\leq \left|1 - \frac{\delta}{\nu}\right| \|\mathbf{E}_\beta\|_V \|\mathbf{E}_\beta - \mathbf{E}\|_V - \mathcal{R}((\mathbf{E}, \mathbf{E}_\beta - \mathbf{E})_W) \end{aligned}$$

Now, the first term in the last inequality tends to 0 according to the assumptions on  $\delta$  and  $\nu$  and since  $(\mathbf{E}_\beta)_\beta$  is bounded in  $W$  and thus in  $V$ . The second term tends to 0 since  $\mathbf{E}_\beta$  converges weakly to  $\mathbf{E}$  in  $W$ . This completes the proof.  $\blacksquare$

### 4.3 Link with Tikhonov regularization

As mentioned in [12], there is a link between the quasi-reversibility method formulated as a mixed problem and standard Tikhonov regularization.

We shall make precise this link for the classical QR-method. To this end, denote by  $A: H(\mathbf{curl}; \Omega) \rightarrow M$  the unique linear continuous operator defined by

$$a(\mathbf{u}, \boldsymbol{\psi}) = (A\mathbf{u}, \boldsymbol{\psi})_{H(\mathbf{curl}; \Omega)} \quad \forall \boldsymbol{\psi} \in M$$

according to the Riesz representation theorem. In the same way, define by  $\mathbf{G} \in M$  the unique Riesz representative of the continuous linear form  $\ell(\cdot)$  such that

$$(\mathbf{G}, \boldsymbol{\psi})_{H(\mathbf{curl}; \Omega)} = \ell(\boldsymbol{\psi}) \quad \forall \boldsymbol{\psi} \in M.$$

Then, the Cauchy problem (6) consists in finding  $\mathbf{E} \in H(\mathbf{curl}; \Omega)$  such that  $\gamma_t \mathbf{E} = \mathbf{f}$  and  $A\mathbf{E} = \mathbf{G}$ .

Now, for a given parameter  $\delta > 0$ , introduce the (real-valued) cost function

$$J_\delta(\mathbf{v}) = \frac{1}{2} \|A\mathbf{v} - \mathbf{G}\|_{H(\mathbf{curl}; \Omega)}^2 + \frac{\delta}{2} \|\mathbf{v}\|_{H(\mathbf{curl}; \Omega)}^2 \quad (28)$$

defined on  $H(\mathbf{curl}; \Omega)$ . The directional derivative of  $J_\delta$  in the direction  $\mathbf{d} \in V_0$  is given by

$$J'_\delta(\mathbf{v})\mathbf{d} = \mathcal{R}((A\mathbf{v} - \mathbf{G}, A\mathbf{d})_{H(\mathbf{curl}; \Omega)}) + \delta(\mathbf{v}, \mathbf{d})_{H(\mathbf{curl}; \Omega)}. \quad (29)$$

Now, let  $(\mathbf{E}_\delta, \mathbf{F}_\delta) \in V_f \times M$  be the solution of the classical QR-problem (7). Then, we get from the second equation of (7) that  $\mathbf{F}_\delta = A\mathbf{E}_\delta - \mathbf{G}$ . Substituting  $\mathbf{F}_\delta$  by this relation in the first equation and taking the real part, yields  $J'_\delta(\mathbf{E}_\delta) = 0$  according to (29) and the definition of  $A$  and  $\mathbf{G}$ . In conclusion, the field  $\mathbf{E}_\delta$  of the unique solution of the QR-method is a critical point of the functional  $J_\delta$  defined by (28).

In the same way, one can show that the field  $\mathbf{E}_\alpha$  of the solution of the relaxed QR method (13) is a critical point of the functional

$$J_\alpha(\mathbf{v}) = \frac{1}{2} \|A\mathbf{v} - \mathbf{G}\|_V^2 + \frac{\eta^2}{2} \|\gamma_t \mathbf{v} - \mathbf{f}\|_{0,\Gamma_0}^2 + \frac{\delta}{2} \|\mathbf{v}\|_V^2$$

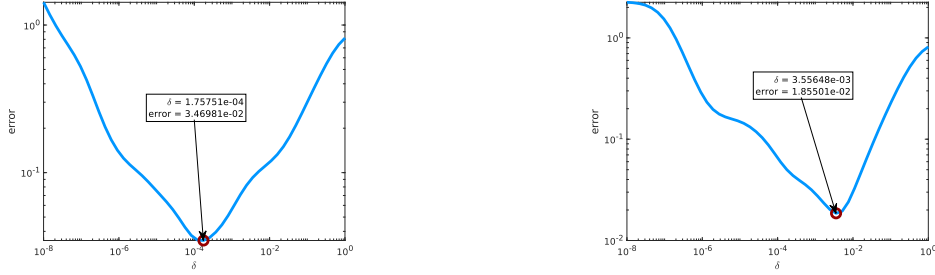


Figure 10: Unit disc. 5% noisy data. RR-QR method. Relative error  $\frac{\|\mathbf{E}-\mathbf{E}_\delta\|_{0,\Omega}}{\|\mathbf{E}\|_{0,\Omega}}$  with respect to the regularization parameter  $\delta$  at fixed  $\eta$  and  $\nu = \delta$ . Left: configuration G34. Right: configuration GE37.

Table 4: Unit disc. 5% noisy data. RR-QR method. Errors in the approximation of  $\mathbf{E}$  for  $\nu = \delta$  at optimal delta and automatically fixed  $\eta$ .

Configuration	$\frac{\ \mathbf{E}-\mathbf{E}_\delta\ _{0,\Omega}}{\ \mathbf{E}\ _{0,\Omega}}$	$\frac{\ (\mathbf{E}-\mathbf{E}_\delta)\times\mathbf{n}\ _{0,\Gamma_0}}{\ \mathbf{E}\times\mathbf{n}\ _{0,\Gamma_0}}$	$\frac{\ (\mathbf{E}-\mathbf{E}_\delta)\times\mathbf{n}\ _{0,\Gamma_1}}{\ \mathbf{E}\times\mathbf{n}\ _{0,\Gamma_1}}$	$\ \mathbf{F}_\delta\ _{0,\Omega}$
G34	3.4698e-02	2.9145e-02	3.5686e-01	7.0667e-03
GE37	1.8550e-02	3.2848e-02	1.7154e-01	1.1857e-02

defined on the vector space  $V$  for a parameter set  $\alpha = (\delta, \eta)$ .

Finally, if we let

$$J_\beta(\mathbf{v}) = J_\alpha(\mathbf{v}) + \frac{\nu}{2}\|\gamma_t\mathbf{v}\|_{0,\Gamma_1}^2,$$

for any  $\mathbf{v} \in W$  and  $\beta = (\delta, \eta, \nu)$ , the field  $\mathbf{E}_\beta$  of the solution of the regularized relaxed QR method (22) is a critical point of  $J_\beta$ .

#### 4.4 Numerical results with noisy data

We use the same physical parameters as in subsection 3.2. In the sequel, we describe the generation of synthetic noisy data. To simplify the notation, we consider here that the input data  $\mathbf{f}$  and  $\mathbf{g}$  are vectors of degrees of freedom. They are perturbed as follows. First, two vectors  $\mathbf{b}_f$  and  $\mathbf{b}_g$  are generated, following a standard normal distribution. Then, the perturbed data  $(\mathbf{f}^p, \mathbf{g}^p)$  are obtained from

$$\mathbf{f}^p = \mathbf{f} + p \frac{\|\mathbf{f}\|}{\|\mathbf{b}_f\|} \mathbf{b}_f, \quad \mathbf{g}^p = \mathbf{g} + p \frac{\|\mathbf{g}\|}{\|\mathbf{b}_g\|} \mathbf{b}_g,$$

where  $p > 0$  is the applied level of noise.

Numerical results are presented for the second version of the regularized relaxed quasi-reversibility (RR-QR) method (22) with  $\nu = \delta$  and  $p = 5\%$  noise. The parameter  $\eta$  is fixed automatically through the following procedure (see [12]). First, we compute the Riesz representative  $\mathbf{G}^p$  of  $\mathbf{g}^p$  in the Hilbert space  $M$  by solving

$$(\mathbf{G}^p, \boldsymbol{\psi})_W = (\mathbf{g}^p, \boldsymbol{\psi})_{0,\Gamma_0}, \quad \forall \boldsymbol{\psi} \in M.$$

Then, we define:

$$\eta = \frac{\|\mathbf{G}^p\|_W}{\|\mathbf{f}^p\|_{L^2(\Gamma_0)}}.$$

First, let  $\Omega$  be the unit disc. In Figure 10 we show the evolution of the error in  $L^2(\Omega)$ -norm with respect to  $\delta$ , for the two configurations of the boundary. For the specific case of  $\delta$  minimizing the error, we show this error over the whole domain in Figure 11 and we list the different errors in Table 4.

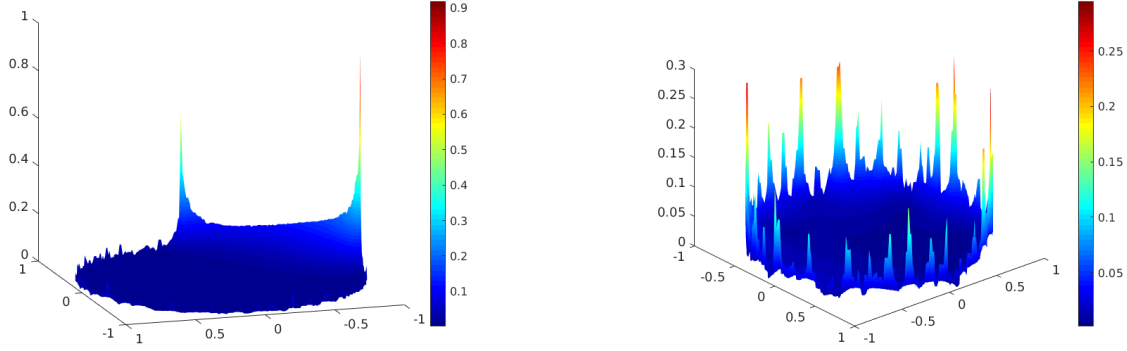


Figure 11: Unit disc. 5% noisy data. RR-QR method. Modulus of the error  $|\mathbf{E} - \mathbf{E}_\beta|$ . Left: configuration G34. Right: configuration GE37.

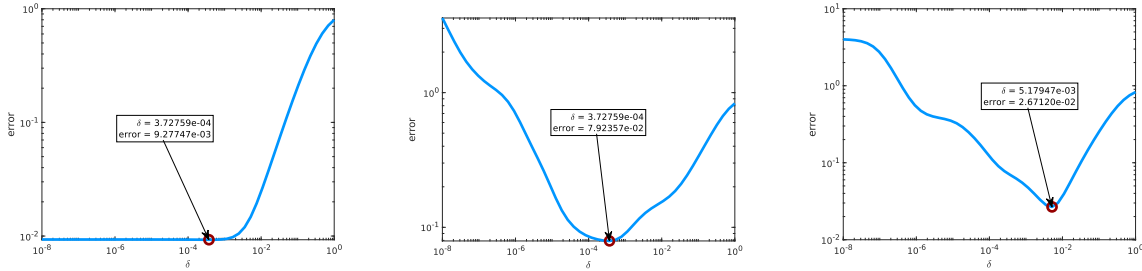


Figure 12: Ring. 5% noisy data. RR-QR method with extension/restriction. Relative error for  $\mathbf{E}$  in  $L^2(\Omega)$ -norm with respect to  $\delta$  for  $\nu = \delta$ .  $\eta$  automatically fixed from noise level.

With the same settings, we now test the regularized relaxed quasi-reversibility method (RR-QR) in the ring with extension/restriction. The relative error in  $\mathbf{E}$  with respect to  $\delta$  is shown in Figure 12. For the optimal values of  $\delta$ , the errors are reported in Table 5 and illustrated in Figure 13. One notices the good performance of the method for the three configurations with errors below 8% in all norms except for configuration G34 on  $\Gamma_1$  where the error amounts to 15%. One notices that the method performs better in the ring configuration than in the unit disc.

#### 4.5 Numerical results in three dimensions

We finally present tests in 3D. The physical settings remain the same as in the previous section, and we generate a noise of 5% in the data. The parameter  $\eta$  is automatically fixed following the above mentioned procedure, and we choose  $\nu = \delta$ .

Table 5: Ring. 5% noisy data. RR-QR method with extension/restriction. Errors in the approximation of  $\mathbf{E}$  for optimal  $\delta$  and  $\nu = \delta$ .  $\eta$  automatically fixed from noise level.

Configuration	$\frac{\ \mathbf{E} - \mathbf{E}_\delta\ _{0,\Omega}}{\ \mathbf{E}\ _{0,\Omega}}$	$\frac{\ (\mathbf{E} - \mathbf{E}_\delta) \times \mathbf{n}\ _{0,\Gamma_0}}{\ \mathbf{E} \times \mathbf{n}\ _{0,\Gamma_0}}$	$\frac{\ (\mathbf{E} - \mathbf{E}_\delta) \times \mathbf{n}\ _{0,\Gamma_1}}{\ \mathbf{E} \times \mathbf{n}\ _{0,\Gamma_1}}$	$\frac{\ (\mathbf{E} - \mathbf{E}_\delta) \times \mathbf{n}\ _{0,\Gamma_1}}{\ \mathbf{E} \times \mathbf{n}\ _{0,\Gamma_1}}$	$\ \mathbf{F}_\delta\ _{0,\Omega}$
GExt	9.2775e-03	3.3871e-02	4.2425e-03	4.2425e-03	1.0602e-02
G34	7.9236e-02	3.0600e-02	1.5695e-01	4.2697e-02	8.7901e-03
GE37	2.6712e-02	3.3503e-02	7.7043e-02	1.6996e-02	1.3596e-02

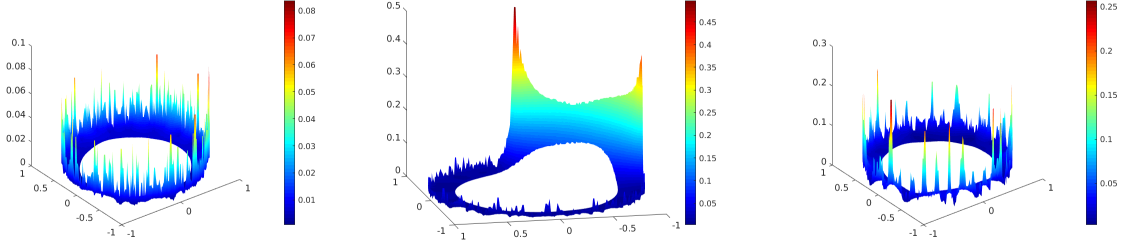


Figure 13: Ring. 5% noisy data. RR-QR method with extension/restriction. Modulus of the error in the approximation of  $\mathbf{E}$  for optimal  $\delta$  and  $\nu = \delta$ .  $\eta$  automatically fixed from noise level. Left: configuration GExt. Middle: configuration G34. Right: configuration GE37.

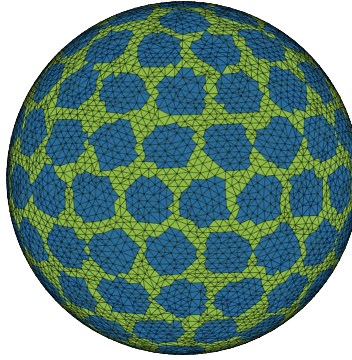


Figure 14: Accessible part  $\Gamma_0$  in 3D configurations. Set of 128 electrodes.

Here, however, the domain  $\Omega$  is a subset of  $\mathbb{R}^3$ . Two domains are tested. The first one is the unit ball of  $\mathbb{R}^3$ , discretized with a mesh size  $h = 1.43e-1$ , ending up with 90 077 tetrahedrons and 114 347 edges. The accessible part,  $\Gamma_0$ , is defined as the union of 128 electrodes covering approximately 61% of the whole boundary. This boundary configuration is illustrated in Figure 14.

The second domain is a ring of width 0.3, defined as the unit ball of  $\mathbb{R}^3$ , minus the ball centered at the origin and of radius 0.7. The mesh size is close to the ball's one:  $h = 1.41e-1$ , ending up with 70 420 tetrahedrons and 96 686 edges. The boundary configuration is the same as for the unit disc: the interior boundary of the ring is part of  $\Gamma_1$  and  $\Gamma_0$  represents here about 41% of the whole boundary. The quasi-reversibility system will be solved in this 3D ring with the extension/restriction method introduced in Algorithm 1.

We show in Figure 15 the evolution of the relative error in  $L^2$ -norm in the whole domain with respect to  $\delta$ . As in the two dimensional cases, the error decreases with  $\delta$ , reaches a minimum, and then increases. Table 6 lists the errors obtained with the value of  $\delta$  realizing this minimum. The error  $\|\mathbf{E}_\delta - \mathbf{E}\|_{0,\Omega}$  is shown in this case in Figure 16.

Table 6: Errors in the unit ball of  $\mathbb{R}^3$  and in a three dimensional ring.

Domain	$\frac{\ \mathbf{E} - \mathbf{E}_\delta\ _{0,\Omega}}{\ \mathbf{E}\ _{0,\Omega}}$	$\frac{\ (\mathbf{E} - \mathbf{E}_\delta) \times \mathbf{n}\ _{0,\Gamma_0}}{\ \mathbf{E} \times \mathbf{n}\ _{0,\Gamma_0}}$	$\frac{\ (\mathbf{E} - \mathbf{E}_\delta) \times \mathbf{n}\ _{0,\Gamma_1}}{\ \mathbf{E} \times \mathbf{n}\ _{0,\Gamma_1}}$	$\frac{\ (\mathbf{E} - \mathbf{E}_\delta) \times \mathbf{n}\ _{0,\Gamma_i}}{\ \mathbf{E} \times \mathbf{n}\ _{0,\Gamma_i}}$	$\ \mathbf{F}_\delta\ _{0,\Omega}$
Ball	1.0834e-01	2.3864e-02	4.0949e-01	.	2.9336e-03
Ring	1.2414e-01	1.1567e-02	2.7969e-01	5.6528e-02	1.6497e-03

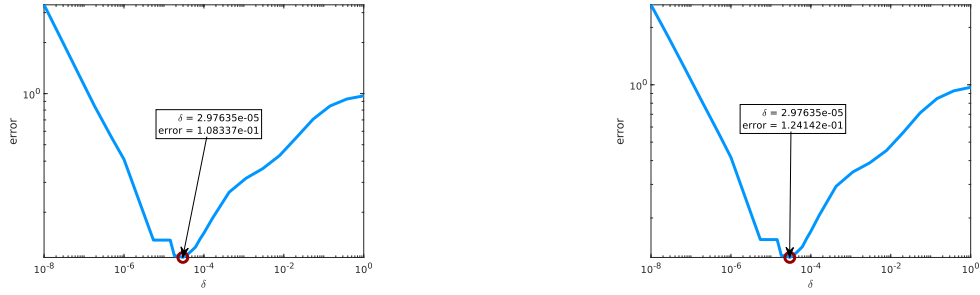


Figure 15: Relative error  $\frac{\|\mathbf{E} - \mathbf{E}_\delta\|_{0,\Omega}}{\|\mathbf{E}\|_{0,\Omega}}$  with respect to the regularization parameter  $\delta$ . Left: Unit ball of  $\mathbb{R}^3$ . Right: 3D ring of internal radius 0.7.

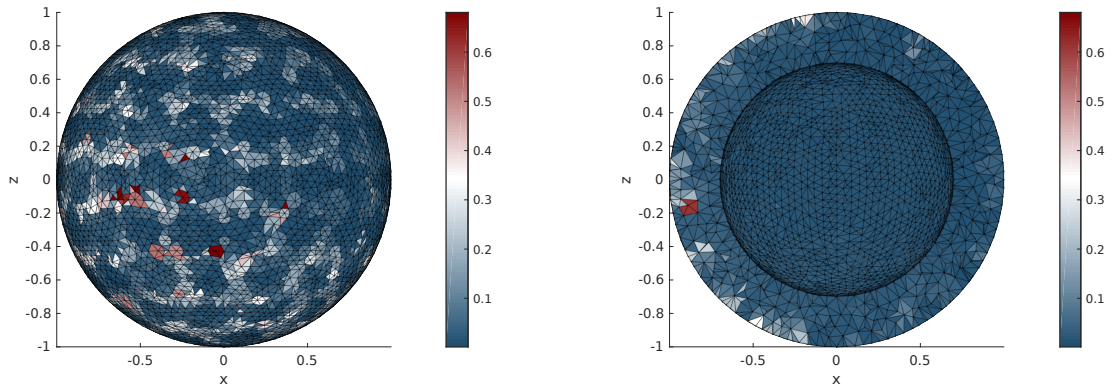


Figure 16: Error in the three-dimensional ring. Left: view of the external boundary. Right: cut showing the internal boundary.

## 4.6 Choice of the regularization parameter. General case.

From the former numerical results, we can attest that the QR-method in its classical or regularized and relaxed version is a reliable tool for data completion and data transmission problems in two and three dimensional configurations.

The choice of the regularization parameter  $\delta$  is crucial for the quality of the approximation. In the former tests, the parameter has been fixed to an optimal value by evaluating the error in the  $L^2(\Omega)$ -norm for each value in a given range. In practice, when the exact solution is not known, this procedure is not possible, but classical strategies as the Morozov's discrepancy principle or the L-curve method can be applied to retrieve a value for  $\delta$ . Here, the L-curve method consists in drawing the graph of  $\|\mathbf{E}_\delta\|_{0,\Omega}$  with respect to  $\|\mathbf{F}_\delta\|_{0,\Omega}$  for different values of  $\delta$ . We then choose  $\delta$  to minimize both norms as much as possible. In Figure 17, we show the L-curve we obtained in the ring with 5% noise for the configuration G37 and the three-dimensional ring. Interestingly, the minimum of the error on  $\Gamma_i$ , highlighted by a circle, is located at the corner of the L-curve, which can then be automatically computed with, for example, the triangle method [18].

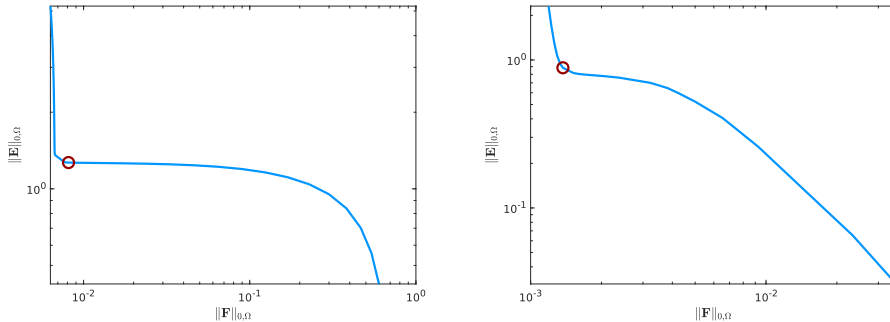


Figure 17: L-curve corresponding to the RR-QR method with extension/restriction in the ring. 5% noisy data. Left: configuration G37 (2D). Right: 3D ring.

The choice of the second regularization parameter  $\nu$  should be made in accordance with Theorem 4.2, i.e.  $\lim_{(\delta,\nu)\rightarrow 0} \frac{\delta}{\nu} = 1$ . Roughly speaking, this amounts to take  $\nu = \delta$ . However, this condition has only been proven to be sufficient to assure the convergence of the RR-QR method, and other choices of  $\nu$  could possibly improve the results. Finally, in all our numerical experiments with the RR-QR method, the relaxation parameter  $\eta$  has been fixed according to the heuristical arguments presented here-above (see [12]). Again, this choice is possibly not optimal and could be improved.

## 5 Conclusion and future works

In this paper, we have addressed two complementary questions relative to the reconstruction of the dielectric coefficients of a medium from partial boundary measurements. The underlying equations are the time-harmonic Maxwell equations formulated in the electric field. First, we have proved an identifiability result which states that identical partial data sets yield identical interior coefficients, assuming that the dielectric properties are known in a neighbourhood of the boundary. This assumption is realistic in many practical applications, and is less restrictive than geometrical or boundary conditions on the inaccessible part of the boundary. Secondly, we have dealt with the issue how to retrieve in a stable way the missing data on the inaccessible part. To this end, we have studied the quasi-reversibility method for the data completion problem. We have proposed different mixed formulations: a classical one, and two regularized relaxed formulations. We have proved their well-posedness and the convergence of the regularized solution to the exact solution under some conditions on the regularization

and relaxation parameters. A large variety of two-dimensional and three-dimensional numerical results attest the efficiency of the method, in particular for noisy data.

This non-iterative data completion procedure would be an interesting initial step for numerical methods to reconstruct the dielectric properties of a tissue or a material. We have in mind, in particular, brain medical applications (e.g. microwave tomography) and the cortical mapping problem which consists in reconstructing from electric potential measurements available at part of the scalp the potential on the inner cortex surface. This question of multi-layer data completion has been studied for Laplace's equation in the context of the EEG (electroencephalography) inverse source localization [20, 21]. To the best of our knowledge, this problem hasn't been treated for electromagnetic inverse medium problems and induces both theoretical and numerical challenging questions. This is part of ongoing work.

## References

- [1] Alessandrini G., Stable determination of conductivity by boundary measurements, *Appl. Anal.*, 27:1-3 (1988), pp. 153–172.
- [2] Alessandrini G., Rondi L., Rosset E. , Vessella S., The stability for the Cauchy problem for elliptic equations, *Inverse problems*, 25 (2009), 123004.
- [3] Ammari H., *Mathematical Modeling in Biomedical Imaging I: Electrical and Ultrasound Tomographies, Anomaly Detection, and Brain Imaging*, Lecture Notes in Mathematics: Mathematical Biosciences subseries, Vol. 1983. Springer-Verlag. Berlin. 2009.
- [4] Ammari H, Garnier J, Kang H, Nguyen L, Seppecher L., *Multi-Wave Medical Imaging: Mathematical Modelling and Imaging Reconstruction, Volume 2*. World Scientific. London. 2017.
- [5] Andrieux S., Baranger T.N., Ben Abda A., Solving Cauchy problems by minimizing an energy-like functional, *Inverse Problems*, 22 (2006), 115.
- [6] Azaïez M., Ben Belgacem F., El Fekih H., On Cauchy's problem: II. Completion, regularization and approximation, *Inverse Problems*, 22 (2006), pp.1307–1336.
- [7] Ben Belgacem F., Why is the Cauchy problem severely ill-posed?, *Inverse Problems*, 23 (2007), pp. 823–836.
- [8] Ben Belgacem F., El Fekih H., On Cauchy's problem: I. A variational Steklov-Poincaré theory, *Inverse Problems*, 21 (2005), pp. 1915–1936.
- [9] Borcea L, Electrical impedance tomography, *Inverse Problems*, 18(6) (2002), pp. R99–R136.
- [10] Bourgeois L., A mixed formulation of quasi-reversibility to solve the Cauchy problem for Laplace's equation, *Inverse Problems*, 21 (2005), pp.1087–1104.
- [11] Bourgeois L., Dardé J., A duality-based method of quasi-reversibility to solve the Cauchy problem in the presence of noisy data, *Inverse Problems*, 26(9) (2010), 095016.
- [12] Bourgeois L., Recoquillay A., A mixed formulation of the Tikhonov regularization and its application to inverse PDE problems, *Mathematical Modelling and Numerical Analysis*, 52(1) (2018), pp.123–145.
- [13] Brown B.M., Marletta M., Reyes J.M., Uniqueness for an inverse problem in electromagnetism with partial data, *J. Differential Equations*, 260 (2016), pp. 6525–6547.
- [14] Calderón A.P., On an inverse boundary value problem, *Seminar on Numerical Analysis and its Applications to Continuum Physics*, Soc. Brasileira de Matemática. Rio de Janeiro. 1980, pp. 65-73.

- [15] Caro P., On an inverse problem in electromagnetism with local data: stability and uniqueness, *Inverse Probl. Imaging*, 5 (2011), pp. 297–322.
- [16] Caro P., García A., Reyes J. M., Stability of the Calderón problem for less regular conductivities, *J. Differential Equations*, 254:2 (2013), pp.469–492.
- [17] Caro P., Zhou T., Global uniqueness for an IBVP for the time-harmonic Maxwell equations, *Anal. PDE*, 7(2) (2014), pp. 375–405.
- [18] Castellanos J.L., Gómez S., Guerra V., The triangle method for finding the corner of the L-curve, *Applied Numerical Mathematics*, 43(4) (2002), pp. 359–373.
- [19] Cimetière A., Delvare F., Jaoua M, Pons F., Solution of the Cauchy problem using iterated Tikhonov regularization, *Inverse problems*, 17 (2001), 553.
- [20] Clerc M., Leblond J., Marmorat J.-P., Papadopoulo T., Source localization in EEG using rational approximation on plane sections, *Inverse Problems*, 28 (2012), 055018.
- [21] Clerc M., Leblond J., Marmorat J.-P., Papageorgakis C., Uniqueness result for an inverse conductivity recovery problem with application to EEG, *Rendiconti dell’Istituto di Matematica dell’Università di Trieste. An International Journal of Mathematics* (2016), 48.
- [22] Dardé J., Iterated quasi-reversibility method applied to elliptic and parabolic data completion problems, *Inverse Problems and Imaging*, 10(2), (2016), pp.379–407.
- [23] Grisvard P., *Singularities in Boundary Value Problems*, RMA 22, Masson, Springer-Verlag, 1992.
- [24] Hecht F., New Development in FreeFem++, *Journal of Numerical Mathematics*, 20(3-4) (2012), pp. 251–265.
- [25] Ola P., Päivärinta L., Somersalo E., *Inverse Problems for Time Harmonic Electrodynamics, Inside Out: Inverse Problems and Applications*, Math. Sci. Res. Inst. Publ., vol. 47, Cambridge University Press, Cambridge, 2003, pp. 169–191.
- [26] Monk P., *Finite Element Methods for Maxwell’s Equations*, Oxford University Press, 2003.
- [27] Kozlov V.A., Mazya V.G., Fomin A.V., An iterative method for solving the Cauchy problem for elliptic equation, *Comput. Math. Phys.*, 31 (1991), pp. 45–52.
- [28] Klibanov M. V., Santosa F., A computational quasi-reversibility method for cauchy problems for Laplace’s equation, *SIAM J. Appl. Math.*, 51 (1991), pp.1653–1675.
- [29] Lattès R., Lions J.-L., *Méthode de Quasi-réversibilité et Applications*, Dunod, Paris, 1967.
- [30] McCann H., Pisano G., Beltrachini L., Variation in Reported Human Head Tissue Electrical Conductivity Values, *Brain Topography* (2019). <https://doi.org/10.1007/s10548-019-00710-2>
- [31] Nédélec J.-C., Mixed finite elements in  $\mathbb{R}^3$ , *Numer. Math.*, 35 (1980), pp. 315–341.
- [32] Somersalo E., Isaacson D., Cheney M., A linearized inverse boundary value problem for Maxwell’s equations, *J. Comput. Appl. Math.*, 42(1) (1992), pp. 123–136.
- [33] Sylvester J., Uhlmann G., A global uniqueness theorem for an inverse boundary value problem, *Ann. of Math. (2)* 125:1 (1987), pp. 153–169.
- [34] Tofighi M.R., Daryoush A., *Measurement Techniques for the Electromagnetic Characterization of Biological Materials*, *Handbook of Engineering Electromagnetics*, CRC Press (2004).

- [35] Tournier P.-H., Aliferis I., Bonazzoli M., de Buhan M., Darbas M., Dolean V., Hecht F., Jolivet P., El Kanfoud I., Migliaccio C., Nataf F., Pichot C., Microwave Imaging of Cerebrovascular Accidents by Using High-Performance Computing, *Parallel Computing*, 85 (2019), pp. 88-97.
- [36] Tournier P.-H., Bonazzoli M., Dolean V., Rapetti, Hecht F., Nataf F., Aliferis I, El Kanfoud I., Migliaccio C., de Buhan M., Darbas M., Semenov S., Pichot C., Numerical Modeling and High Speed Parallel Computing: New Perspectives for Tomographic Microwave Imaging for Brain Stroke Detection and Monitoring, *IEEE Antennas and Propagation Magazine*, 59(5) (2017), pp. 98-110.
- [37] Uhlmann G., Electrical impedance tomography and Calderón's problem, *Inverse Problems*, 25:12 (2009), 123011.